IEICE TRANS. COMMUN., VOL.E105–B, NO.10 OCTOBER 2022

PAPER

Non-Destructive Inspection of Twisted Wire in Resin Cover Using Terahertz Wave

Masaki NAKAMORI[†a)], **Yukihiro GOTO**[†], **Tomoya SHIMIZU**[†], *and* **Nazuki HONDA**[††], ***Members***

SUMMARY We proposed a new method for evaluating the deterioration of messenger wires by using terahertz waves. We use terahertz time-domain spectroscopy to measure several twisted wire samples with different levels of deterioration. We find that each twisted wire sample had a different distribution of reflection intensity which was due to the wires' twist structure. We show that it is possible to assess the degradation from the straight lines present in the reflection intensity distribution image. Furthermore, it was confirmed that our method can be applied to wire covered with resin.

key words: *terahertz time-domain spectroscopy, non-destructive inspection, messenger wire, deterioration*

1. Introduction

To provide telecommunication services, NTT has installed a large number of facilities such as utility poles and telecommunication cables [1]. Figure 1 shows an example of the configuration of optical communication equipment in NTT access networks. The access section of the communication network consists of aerial lines for safe and reliable individual distribution. The messenger wire supports the tension applied to the cable and self-weight. The support wire supports the tension applied to the utility pole to maintain a balance of tension. Unfortunately, in harsh outdoor environments, wires rust and rapidly deteriorate. These outdoor facilities are visually inspected by on-site workers regularly. However, the number of on-site workers will decrease due to the fall in Japan's working population [2] soon. To address this impending problem, we must improve the productivity and efficiency of maintenance work.

Messenger wire and support wire are made of twisted steel wires. Steel wires have high weather resistance, but the surface of the wires sometimes can rust and wear out over time, lowering their durability. Eventually, the wires are liable to break because they cannot withstand the weight and tension of cables. In current inspection regimes, the messenger wire and support wire are diagnosed by appearance, and more recently, photographs have been used for more efficient inspections.

It is very important to be able to inspect the facilities nondestructively so as not to degrade their durability. The progression of rust (hereafter referred to as deterioration) is mainly judged from the color of the photographed wires [3]. However, it is not always possible to accurately distinguish deterioration from just color since color can change due to imaging conditions such as backlighting from the sun. In addition, some messenger wires and support wires are resin-covered which precludes being photographed. To solve these problems, it is necessary to develop a non-destructive inspection technology that is not affected by backlighting and can inspect the wires even when covered.

Terahertz (THz) waves have been attracting attention as they offer many useful applications. THz waves are electromagnetic waves with frequencies ranging from 0.1 to 10 THz. They offer good penetration of non-conducting materials [4]. The performance of devices and products for THz wave applications continues to improve. They are now used in many fields such as chemical production [5], communications [6], and industry [7]. Non-destructive inspection technologies are also being actively studied [4], [8]. Examples reported to date include the detection of gaps in a tunnel wall [9] and rust under a painted surface [10]. THz waves are not affected by backlight as they lie outside the frequency band of natural light. Therefore, we expect THz waves will be useful for inspecting messenger wires or support wires in terms of permeability and environmental robustness.

However, the response of THz waves to the deterioration of twisted wires, such as messenger wires and support wires, has not been studied in detail. In this study, we use terahertz time-domain spectroscopy (THz-TDS) [11] to clarify their response to twisted wire deterioration and introduce a method for distinguishing the extent of deterioration. We measure five twisted wire samples with varying levels of deterioration using THz-TDS and determine that the reflection intensity distribution of each sample is different. We show that it is possible to distinguish deteriorated twisted wires from the straight lines formed in the reflection intensity distribution image that represent the individual wire strands. Previous studies have investigated the detection of rust. In this study, we propose a method for distinguishing twisted wire whose durability decreases remarkably by corrosion.

The rest of this paper is organized as follows. Section 2 introduces the measurement method and the samples used, and Sect. 3 describes the measurement results and the method of identifying deteriorated twisted wire. Finally, Sect. 4 summarizes this paper.

Manuscript received August 27, 2021.
Manuscript revised December 24, 2021.
Manuscript publicized April 13, 2022.

[†]The authors are with Access Network Service Systems Laboratories, NTT Corporation, Tsukuba-shi, 305-0805 Japan.
[††]The author is with Technical Assistance and Support Center, NTT EAST, Tokyo, 144-0053 Japan.
a) E-mail: masaki.nakamori.xk@hco.ntt.co.jp

DOI: 10.1587/transcom.2021EBP3138

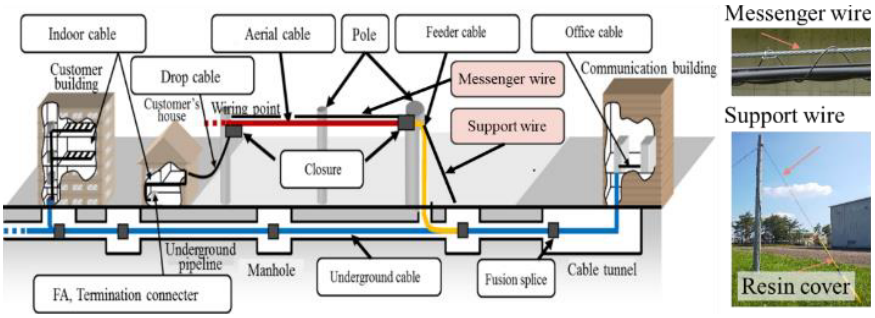

Fig. 1 Configuration of outdoor telecommunications facilities in Japan.

2. Equipment

2.1 Measurement Setup

The response of THz waves to twisted wires and resin covers is not known well. Accordingly, we applied THz-TDS over a wide range of frequencies instead of a single frequency. The THz-TDS measurement system used in this study is shown in Fig. 2. THz-TDS is a material analysis method that can directly observe THz pulse waveforms in the time domain and obtain spectral information in the frequency domain by using Fourier transform. A femtosecond laser is split into a pump light and a probe light and directed to the THz wave generator and the detector, respectively. Here, the wavelength is 785 nm and the pulse width is 86 fs. The waveform of the femtosecond laser pulse is Gaussian. After the THz waves are reflected from the sample, they pass through the beam splitter (BS) and are incident on the detector. THz waves are detected only when they are incident at the same time as the probe light. The waveform of the THz waves can be obtained by shifting the timing at which the probe light reaches the detector by using a delay line. We use a single-cycle pulse as shown in the upper right corner of Fig. 2. The pulse width of the generated THz wave was 0.2 ps and had an optimal depth resolution of about 30 μm. The pulse bandwidth ranged from 0.3 to 3.5 THz and the center frequency was about 0.5 THz. The focal length of the lens is 100 mm. The spot size at the focal point was about 0.54 to 6.3 mm and the typical value at 1 THz is 1.9 mm. The diameter of the twisted wire is about 7 mm, making it large enough to obtain a reflected wave.

The shape of the twisted wire is not planar so the reflected wave varies depending on the measuring point. In this measurement, the twisted wire was rotated and moved in the longitudinal direction to obtain the waveform at each point on the surface of the wire. In practice, the rotation and measurement were performed alternately. When the measurement in the rotational direction was finished, the position in the longitudinal direction was moved and the same measurement was repeated. The twisted wire was moved horizontally from 0 to 15 mm in 1 mm steps and rotated from 0 to 90° in 1° steps.

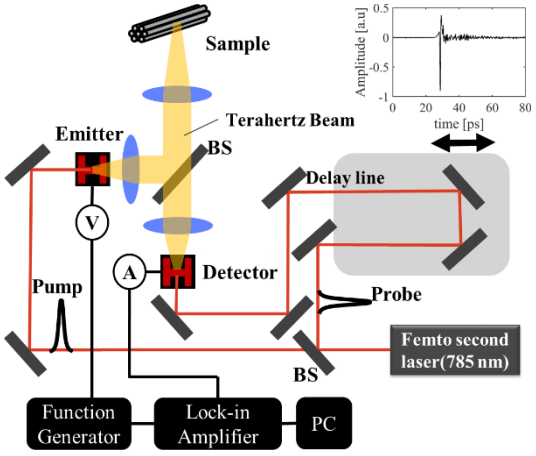

Fig. 2 Experimental setup of THz-TDS.

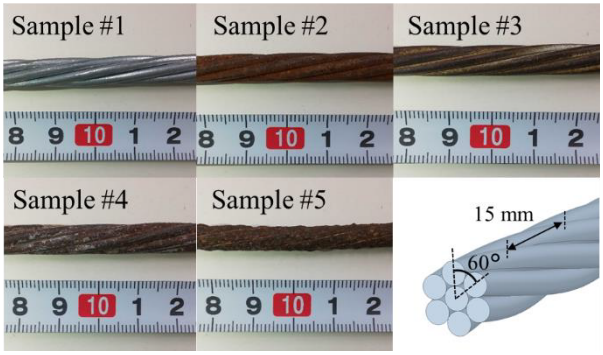

Fig. 3 Twisted wire samples.

2.2 Twisted Wire Samples

We prepared five twisted wire samples with different levels of deterioration as shown in Fig. 3. Sample #1 is an unused wire while sample #5 is the most deteriorated one. Samples #2, #3, and #4 correspond to intermediate levels of deterioration between samples #1 and #5. The twisted wires are made of seven steel wires, each 2.3 mm in diameter. A cross-sectional view of a typical twisted wire is shown in the lower right of Fig. 3. The wire bundles have a twist interval of 60°. In the longitudinal direction, the pitch of each wire is about 15 mm. Plating, usually zinc, is applied to cover

the entire surface of each strand of the twisted wire. The twisted wire begins to corrode at the plating. The corrosion on the plating prevents rust from forming on the steel which is the main material. When the plating is removed, the steel is exposed and corrosion of the steel progresses. The wires wear down and the surface becomes rough as the steel rusts. As corrosion progresses, the surface color changes from red to black. The samples shown in Fig. 3 are arranged in advancing order of deterioration, showing the change of color as the deterioration advances from sample #1 to #5. Sample #5 is of particular concern with regard to decreased durability.

3. Measurement Result and Discussion

The goal of degradation discrimination is to reliably identify the twisted wires that need to be replaced immediately, sample #5 in this case.

3.1 Measurement Result

Figure 4 shows the intensity distribution of the THz waves reflected from the twisted wires. The graphs plot the results of samples #1 to #5. The horizontal and vertical axis represents the wire length in the longitudinal direction and the rotation angle, respectively. The color represents the reflection intensity. The reflection intensity is an absolute value of the maximum amplitude intensity of the waveform pulse reflected from each point. Figure 4 shows that the distribution of reflection intensity in samples #1 to #4 is regular. On the other hand, we confirmed that the distribution of reflection intensity in sample #5 is irregular. We also observed that the reflection intensity was highest in sample #1 and lowest in sample #5. At 1.5 THz or more, the reflected wave was weaker than the light-receiving sensitivity of the measuring instrument and so was not detected. We discuss the cause of this intensity distribution and the decrease in reflection intensity. The surface roughness tends to increase as the deterioration progresses. Samples #1 to #5 are arranged in descending order of roughness and deterioration proceeds in this order as well. Figure 4 shows that the interval between regions having high reflection intensity is about 60 degrees. According to Fig. 3 this value matches the interval of the steel wire strands that make up the twisted wire. The reflection intensity increases because the angle of incidence at the apex of the twist structure is close to perpendicular. Note that the twist structure of sample #5 cannot be confirmed because the surface is heavily worn and it has been lost. Thus, the regular distribution of reflection intensity in samples #1 to #5 is likely caused by the twist structure.

Next, we examined the cause of the decrease in reflection ratio with deterioration. As mentioned previously, the surface tends to become rough as deterioration progresses. The frequency characteristics of the reflection ratio of THz waves for a plane with surface roughness have been reported [12] and are expressed by Eq. (1).

$$\frac{R}{R_0} = \exp\left(-\left(\frac{4\pi f\sigma}{c}\right)^2\right) \tag{1}$$

where R is the effective reflectance, R_0 is the reflectance from a layered perfectly reflecting surface such as a mirror, f is the frequency, σ is the surface roughness, and c is the speed of light. The surface roughness is the root-mean-square (rms) roughness. Fig. 5 shows the relationship between the reflection ratio and the roughness of each sample. The reflection ratio R/R_0 is calculated as the square of the ratio of reflection amplitude of each sample to that of the reflection mirror. Here, we calculated using the highest reflection amplitude at the apex of the twist structure. The apex here is the highest point of convexity among the bumps created by the neighboring wires as seen from the center of the twisted wire. The apex of the twist structure is not a

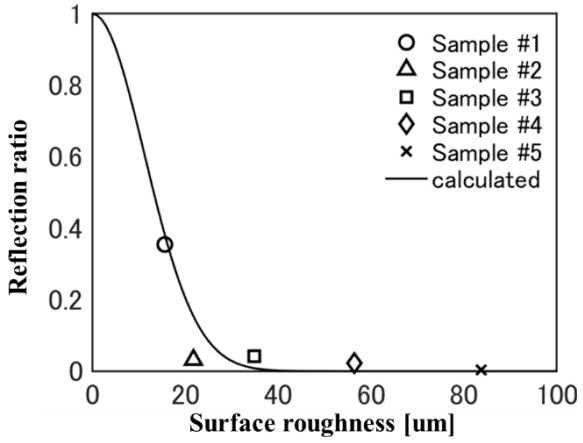

Fig. 5 Relationship between reflection ratio and surface roughness.

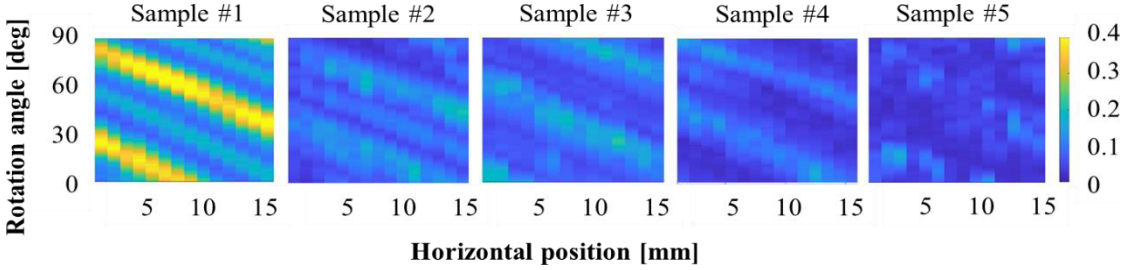

Fig. 4 Reflection intensity distribution from each twisted wire sample.

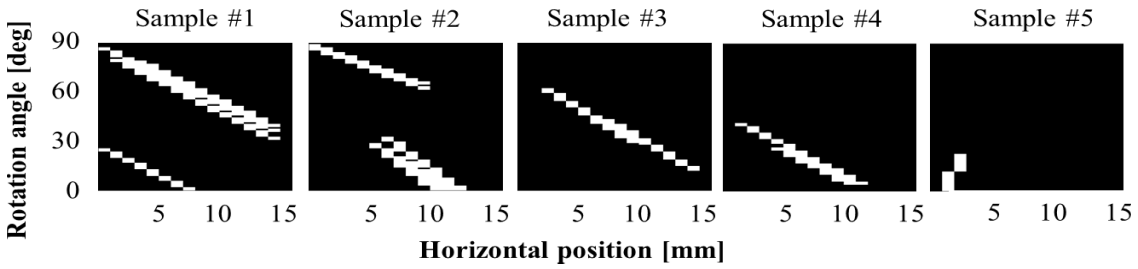

Fig. 6 Example of linear detection results for each sample.

plane but a curved surface. Equation (1) is given for a planar configuration. To reduce the effect of curved surfaces, it is preferable to use higher frequencies where the beam diameter is as small as possible. Therefore, we calculated using the value of 1.5 THz. The reflection intensity at 1.5 THz was calculated by Fourier transforming the reflection waveform. The solid line indicates the results calculated using Eq. (1). The plots show actual measurement results. The surface roughness is the rms roughness measured by a microscope. The reflection ratio tends to decrease as the surface roughness increases. We determined that this tendency closely resembles the calculated results. Therefore, the decrease in the reflection ratio shown in Fig. 4 is due to the rough surface caused by rust. Although there is a correlation between surface roughness and reflection ratio, it is difficult to distinguish between samples #2, #3, #4, and #5 by using only the reflection ratio.

3.2 Method for Distinguishing Deteriorated Samples

We focused on the intensity distribution in order to quantitatively judge the progress of deterioration in the twisted wires. The intensity distribution is characterized by the twist structure. We developed a method for visualizing the intensity distribution and extracting the linear component corresponding to the twist structure to extract this feature. The twist structure becomes unclear as the deterioration progresses. Thus, the characteristics of the extracted straight lines are expected to depend on the sample. The results of the intensity distributions in each sample are first normalized by the maximum value of the reflection intensity. The normalized results are then binarized at some threshold. Finally, straight-line detection was performed on the binarized images.

We used the Hough transform to detect the straight lines. The Hough transform is a well-known algorithm for detecting straight lines. There are mainly two methods, Standard Hough Transform (SHT) [13] and Progressive Probabilistic Hough Transform (PPHT) [14]. The method using SHT is not capable of detecting line segments. So, we adopt the Progressive Probabilistic Hough Transform, which is capable of detecting line segments, as suitable for line segment detection for identifying deterioration. Two parameters, minimum line length and maximum line gap are set for line detection using PPHT. The minimum line length determines the minimum length of the detected line. The maximum line gap

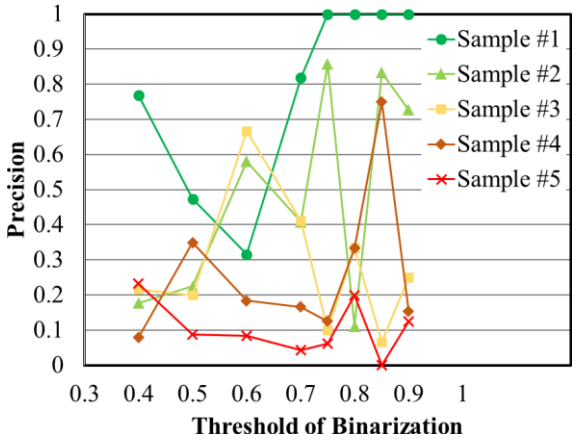

Fig. 7 Relationship between binarization threshold and precision.

Table 1 Number of detected line and correct line.

Threshold	Total number of detected line	Number of correct line
0.5	19	9
0.6	19	6
0.7	11	9
0.8	7	7

is the maximum distance between two lines when they are considered to be one line.

The number and shape of the straight lines detected by the Hough transform were confirmed. Figure 6 shows examples of the straight lines detected from the intensity distribution of samples #1 to #5. Here, we set a threshold of binarization to 0.8, the minimum line length to 5, and the maximum line gap to 2. These values are dimensionless. The white squares show the parts detected as straight lines. From Fig. 6, it can be seen that some straight lines are detected from samples #1 to #4 but fewer in sample #5. In addition, straight lines at a uniform angle were detected in samples #1 to #4. These straight lines were considered to be caused by the twist structure.

We thought that the angle of the detected line could determine whether the straight line was due to twist structure or not. We detected and evaluated a straight line with the correct angle. The precision is the ratio of the number of detected straight lines to the number of straight lines whose angle is the correct value. The pitch was 15 mm and the wire strands are rotated by 60 degrees in actual twisted wire. So, the slope of the straight line detected on the image becomes

−4 degrees/mm in this experiment. The slope of the line varies depending on the selection of pixels. We set the value of −8 to 0 degree/mm as the range of correct inclination, which is double the range of −4 degree/mm. A line that falls within this range is counted as a correct line and a line that does not fall within this range is counted as a miss-detected line. To increase the number of detected lines, the minimum line length was set to 5. Figure 7 shows the relationship between the threshold of binarization and precision. We find that the precision varies with the threshold of binarization from Fig. 7. The precision becomes small at a certain threshold for samples #1 to #4. This is caused by the fact that the width of the line obtained as a result of binarization is the same as the minimum detection length so multiple vertical lines are detected. Table 1 shows the number of detected lines and correct lines corresponding to the threshold of binarization. There is no deterioration and the twist structure is clear in sample #1, so many straight lines are detected when the threshold is low. On the other hand, there are many miss detections so precision is low. The binarization process is carried out in order to emphasize the relatively high-intensity part of each image as an edge. In other words, the apex of the twist structure is extracted. Because the degree of deterioration depends on the twist arrangement, the optimal threshold value also depends on the sample. If the threshold is not optimal, areas that are not part of the twist structure are also extracted, resulting in more false detection. It is difficult to determine the optimal threshold and distinguish the deterioration by using the precision determined at only one threshold of binarization. In order to evaluate the rust progression, we focused on the maximum value of the precision for each sample through the whole binarization range (0.4–0.9). For example, the maximum value of the precision for sample #5 was 0.21 at the highest. On the other hand, for sample #1-4, maximum precisions reach to more than 0.6. Only for sample#5 did the precision fail to become higher regardless of the threshold value. Therefore, it is possible to identify the deterioration by using this fact.

3.3 Distinguishing with Covered Samples

In Sect. 3.2, a method for distinguishing the samples was introduced for a twisted wire without a resin cover. The main advantage of using THz waves is that they can penetrate opaque materials. In this section, we show that this method can be used to distinguish the wires even if they are covered. We examined whether sample #5 could be distinguished by line detection from the intensity distribution obtained by passing through the cover. Using the experimental setup shown in Fig. 2, we set a piece of resin cover 1 cm in front of the measurement sample and measured the reflection intensity. The size of the resin cover was 7.5 cm × 5 cm in a rectangular shape. Figure 8 shows the measurement results of the same samples #1 to #5. After passing through the cover, the intensity of the time waveform was attenuated by about 50 to 60% of that without the cover. Figure 8 shows the intensity distribution of each sample following that in Fig. 2. The intensity distribution due to the twist structure was confirmed in samples #1 to #4 as in the case without the cover.

It was also found that the intensity distribution due to the twist structure could not be confirmed in sample #5. We performed binarization and line detection on these measurement results. Figure 9 plots the relationship between the threshold of binarization and precision with a resin cover. In Fig. 9, the maximum value of the precision for samples #1-4 was 0.6 or higher as same as without cover. The maximum precision value of sample #5 was 0.43, which was not as high as the other samples. The reason for the higher precision of sample#5 compared to the case without resin is thought to be the signal-to-noise ratio. In the normalization process before binarization, the signal intensity is divided by the maximum intensity. The signal from sample #5 has a low signal-to-noise ratio, and the signal-to-noise ratio becomes even lower when the wire is covered. When normalization is performed, the value of the intensity distribution becomes relatively large. As a result, the number of twist structures detected by the binarization is considered to increase. As shown in Sect. 3.2, it can be confirmed that the precision of sample#5 did not increase at any threshold. Therefore, it is possible to use the same algorithm to discriminate between samples with and without cover.

3.4 Discussion

Distribution measurement of twisted wire samples using THz waves was carried out. The results showed that there was a difference in the intensity distribution in the samples.

The decrease of the intensity distribution was also found to be due to surface roughness caused by corrosion. The

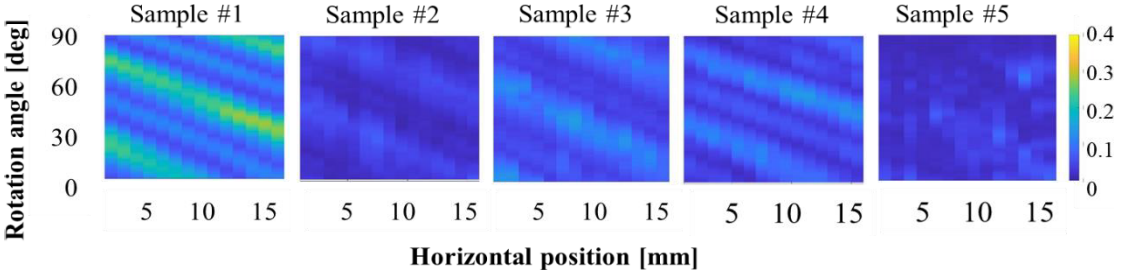

Fig. 8 Reflection intensity distribution from each twisted wire sample with resin covering.

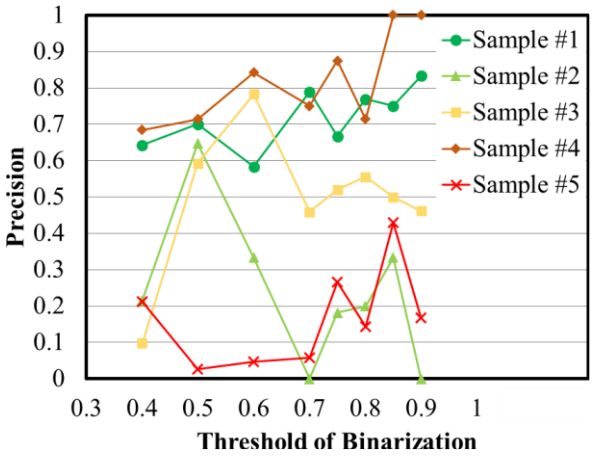

Fig. 9 Relationship between binarization threshold and precision with resin cover.

difference in intensity distribution was used to extract the features of the twist structure. Specifically, line detection was used to extract features corresponding to the twist structure and quantified based on precision. Since the precision depends on the threshold of binarization, it is not possible to determine the degree of deterioration with a single threshold. On the other hand, the most degraded samples showed low precision regardless of the value of the threshold. This tendency was observed regardless of whether or not the sample was covered. Therefore, if no increase in precision can be confirmed even if the threshold value is changed, it can be judged that the sample badly deteriorates. For example, by setting the threshold value of precision to 0.43, sample #5 can be distinguished in which deterioration is significant. In this method, all processes other than the surface measurements to obtain the intensity distribution can be performed by signal processing. Therefore, when this method is applied in actual evaluations, only the surface measurement need be performed in the field, and the rest can be performed by post-processing. The current issue is that the threshold of precision for discrimination is not clear, and we would like to increase the number of samples to clarify the threshold. Another issue is that measurements are possible only at short distances; it is necessary to improve the measurable distance and range so messenger wires at high locations can be assessed.

4. Conclusion

To realize a non-destructive inspection technology that is not affected by environmental lighting effects, we developed a method of using terahertz time-domain spectroscopy to distinguish the extent of deterioration in twisted wires such as messenger wires and support wires. We verified that the response of the reflection intensity distribution was different for twisted wires with different levels of deterioration. We clarified that details of the distribution were determined by the twist structure and surface roughness. In addition, we proposed a method to distinguish the deteriorated twisted wire by detecting straight lines (individual wire strands) from the reflection intensity distribution image. This method makes it possible to determine which twisted wires are heavily degraded regardless of the presence or absence of a cover by obtaining the values of the precision measured while changing the threshold of binarization. Furthermore, this method can be used to determine the messenger wires that need to be replaced, contributing to more efficient inspection in the future.

References

[1] NTT, "The NTT Group promotes efficient resource utilization," https://group.ntt/en/environment/whatdoing/recycling01.html, accessed Nov. 24. 2021.
[2] Statistics Bureau of Japan, "STATISTICAL HANDBOOK OF JAPAN 2020," https://www.stat.go.jp/english/data/handbook/pdf/2021all.pdf#page=1, accessed Nov. 24. 2021.
[3] V. Bondada, D.K. Pratihar, and C.S. Kumar, "Detection and quantitative assessment of corrosion on pipelines through image analysis," Procedia Computer Science, vol.133, pp.804–811, 2018. DOI: 10.1016/j.procs.2018.07.115
[4] S. Zhong, "Progress in terahertz nondestructive testing: A review," Front. Mech. Eng, vol.14, no.3, pp.273–281, 2019. DOI: 10.1007/s11465-018-0495-9
[5] K. Kawase, Y. Ogawa, Y. Watanabe, and H. Inoue, "Non-destructive terahertz imaging of illicit drugs using spectral fingerprints," Opt. Express, vol.11, no.20, pp.2549–2554, 2003. DOI: 10.1364/OE.11.002549
[6] T. Kleine-Ostmann and T. Nagatsuma, "A review on terahertz communications research," J. Infrared, Millim. Terahertz Waves, vol.32, pp.143–171, 2011. DOI: 10.1007/s10762-010-9758-1
[7] M. Yahyapour, A. Jahn, K. Dutzi, T. Puppe, P. Leisching, B. Schmauss, N. Vieweg, and A. Deninger, "Fastest thickness measurements with a terahertz time-domain system based on electronically controlled optical sampling," Appl. Sciences, vol.9, no.7, pp.1283–1294, 2019. DOI: 10.3390/app9071283
[8] Y.H. Tao, A.J. Fitzgerald, and V.P. Wallace, "Non-contact, non-destructive testing in various industrial sectors with terahertz technology," Sensors, vol.20, no.3, pp.712–733, 2020. DOI: 10.3390/s20030712
[9] H. Momiyama, Y. Sasaki, I. Yoshimine, S. Nagano, T. Yuasa, and C. Otani, "Improvement of the depth resolution of swept-source THz-OCT for non-destructive inspection," Opt. Express, vol.28, no.8, pp.12279–12293, 2020. DOI: 10.1364/OE.386680
[10] N. Fuse and K. Sugae, "Non-destructive terahertz imaging of alkali products in coated steels with cathodic disbanding," Prog. Org. Coat., vol.137, pp.105334–105345, 2019. DOI: 10.1016/j.porgcoat.2019.105334
[11] J. Neu and C. Schmuttenmaer, "Tutorial: An introduction to terahertz time domain spectroscopy (THz-TDS)," J. Appl. Phys., vol.124, no.23, pp.1–15, 2018. DOI: 10.1063/1.5047659
[12] T. Fukuchi, N. Fuse, M. Mizuno, and K. Fukunaga, "Surface roughness measurement using terahertz waves," Proc. 3rd ICIAE, pp.294–299, 2015. DOI: 10.12792/iciae2015.053
[13] R.O. Duda and P.E. Hart, "Use of the hough transformation to detect lines, and curves in pictures," Commun. ACM, vol.15, no.1, pp.11–15, 1972.
[14] C. Galamhos, J. Matas, and J. Kittler, "Progressive probabilistic Hough transform for line detection," Proc. Comput. Soc. Conf. Comput. Vision Pattern Recognition, vol.1, pp.554–560, 1999. DOI: 10.1109/CVPR.1999.786993

Masaki Nakamori received the B.E. and M.E. degrees in University of Electro-Comunications, Tokyo, Japan in 2017 and 2019, respectively. He joined NTT Access Network Service Systems Laboratories, Ibaraki, Japan, in 2019. He engaged in research on maintenance and inspection technologies for optical access networks. He is a Member of the Institute of Electronics, Information and Communication Engineers of Japan.

Yukihiro Goto received the B.E., M.E., and Ph.D. degrees in electrical engineering from Osaka Prefecture University, Sakai, Japan, in 2006, 2008 and 2019, respectively. In 2008, he joined NTT Access Network Service Systems Laboratories, Tsukuba, Japan, where he currently engage in research on maintenance and inspection technologies for optical access networks. He is a Member of the Institute of Electronics, Information and Communication Engineers of Japan.

Tomoya Shimizu received B.E. and M.E. degrees in electronic engineering from Tohoku University, Sendai, Japan, in 2000 and 2002, respectively. In 2002, he joined NTT Access Network Service Systems Laboratories, Tsukuba, Japan, he engaged in research on maintenance and inspection technologies for optical access network. He is a member of the Institute of Electronics, Information and Communication Engineers (IEICE) of Japan, and the Japan Society of Applied Physics.

Nazuki Honda received the B.E., M.E., and Ph.D. degrees in electrical and computer engineering from Yokohama National University, Kanagawa, Japan, in 1996, 1998, and 2010, respectively. In 1998, she joined NTT Access Network Service Systems Laboratories, Ibaraki, Japan. She is currently involved in research and development activities for network operations and management in NTT East. Dr. Honda is a Member of the Institute of Electrics, Information and Communication Engineers of Japan.